Information-signal-transfer rate and energy loss in coupled vortex-state networks

Ji-Hye Kim, Ki-Suk Lee, Hyunsung Jung, Dong-Soo Han, and Sang-Koog Kim

Citation: Applied Physics Letters **101**, 092403 (2012); doi: 10.1063/1.4748885

View online: http://dx.doi.org/10.1063/1.4748885

View Table of Contents: http://scitation.aip.org/content/aip/journal/apl/101/9?ver=pdfcov

Published by the AIP Publishing

Information-signal-transfer rate and energy loss in coupled vortex-state networks

Ji-Hye Kim, Ki-Suk Lee,[a] Hyunsung Jung, Dong-Soo Han, and Sang-Koog Kim[b]
National Creative Research Center for Spin Dynamics & Spin-Wave Devices, and Nanospinics Laboratory, Research Institute of Advanced Materials, Department of Materials Science and Engineering, Seoul National University, Seoul 151-744, South Korea

(Received 14 July 2012; accepted 16 August 2012; published online 28 August 2012)

We employed analytical and micromagnetic numerical calculations to elucidate coupled-vortex-gyration-enabled information-signal transfer and the related energy attenuation between vortex-state nanodisks. Specifically, we explored the vortex-gyration transfer rate and the energy attenuation coefficient in terms of the material parameters and dimensions of the coupled disks. Both the micromagnetic simulation and analytical results indicated that the transfer rate is determined by the relative polarization configuration, the saturation magnetization M_s, the radius (R)-to-thickness (L) ratio (R/L) of the given magnetic disks, and the interdistance, whereas the energy attenuation is governed by the intrinsic damping constant as well as the values of M_s, L, and R of the single disks. This work provides a foundation for manipulation of the technologically essential parameters in signal processing, namely speed and energy loss, based on coupled vortex-state networks. © *2012 American Institute of Physics*. [http://dx.doi.org/10.1063/1.4748885]

In the modern electronic devices, information-signal processing is based on the motion of electron charges. On the other hand, several concepts[1–11] entailing magnetization orientations also have been proposed. For example, moving domain walls,[5] propagating spin waves in nanowires,[6–9] and one- and two-dimensional (1D and 2D) magnonic crystals[10,11] can be used as basic elements of information-signal processing. The utilization of the magnetization orientations of nanomagnets offers the benefit of endless switchable magnetization without any translational motion of massive particles.

As an alternative mechanism of information-signal transport, coupled vortex oscillations in vortex-state networks have recently been proposed.[12–16] The magnetic vortex, which is characterized by in-plane curling magnetizations (chirality, C) and out-of-plane magnetizations (polarization, p) in the central region, has a characteristic translational mode (known as *gyration*): a vortex core orbits around its equilibrium center position at a characteristic eigenfrequency ranging from 10 MHz to 1 GHz according to the dot dimensions.[17] During the gyration, the vortex core shifted from its center position leads to non-zero side-surface charges, thus producing stray fields around the dot itself. When another neighboring dot is placed sufficiently close to the first dot, the stray field is strong enough to affect it as well. The rotating stray field has the same frequency as the eigenfrequency ω_0 of the gyration. As reported earlier, such dynamic dipolar interaction causes mutual energy transfer between two coupled vortex oscillators, as between two coupled spring-mass oscillators or pendulums.[13,15,18–21]

Higher operating speed and lower energy dissipation being the most essential factors in information-signal processing technologies, in the present study, we investigated gyration transfer time τ_{ex} and its related energy attenuation coefficient β. We explored, by both micromagnetic simulations and analytical derivations, explicit forms of τ_{ex} and β in terms of their materials parameters, the damping constant α and the saturation magnetization M_s, and the dimensions of a given coupled vortex-state network (radius R, thickness L, and center-to-center interdistance d_{int}).

We used a model of coupled harmonic vortex oscillators composed of two Permalloy (Py) disks [see Fig. 1(a)]. For the purpose of micromagnetic numerical calculations, we employed the OOMMF code,[22] which utilizes the Landau-Lifshitz-Gilbert (LLG) equation of motion for individual magnetizations $\mathbf{M}$: $\partial\mathbf{M}/\partial t = -\gamma(\mathbf{M}\times\mathbf{H}_{eff}) + \alpha/M_s(\mathbf{M}\times\partial\mathbf{M}/\partial t)$ with the gyromagnetic ratio γ and the effective field $\mathbf{H}_{eff}$. Typical material parameters for Py were applied: $M_s = 8.6\times10^5$ A/m, exchange stiffness $A_{ex} = 1.3\times10^{-11}$J/m, $\alpha = 0.01$, $\gamma = 2.21\times10^5$ m/As, and zero magnetocrystalline anisotropy. The unit cell was $3\times3\times L$ nm^3 in size. The upward and downward core orientations in both disks were represented by the vortex polarization, $p=+1$ and $p=-1$, respectively, and the counter-clockwise (CCW) and clockwise (CW) in-plane curling magnetizations were indicated by the chirality, $C=+1$ and -1, respectively. To excite vortex gyration only in disk 1, the initial center position of its core was displaced in the $+y$ direction by application, only to this disk, of a magnetic field in the $+x$ direction. After turning off the field, the vortex-core position vectors of both disks, under free relaxation but coupled to each other, were monitored to extract their motion trajectories.

In order to analytically derive the two parameters of τ_{ex} and β in terms of α, M_s, L, R, and d_{int}, we used the coupled linearized Thiele's equations[23]

$$\begin{aligned} -\mathbf{G}_1\times\dot{\mathbf{X}}_1 - \hat{D}\dot{\mathbf{X}}_1 + \partial W(\mathbf{X}_1,\mathbf{X}_2)/\partial\mathbf{X}_1 = 0,\\ -\mathbf{G}_2\times\dot{\mathbf{X}}_2 - \hat{D}\dot{\mathbf{X}}_2 + \partial W(\mathbf{X}_1,\mathbf{X}_2)/\partial\mathbf{X}_2 = 0, \end{aligned} \quad (1)$$

[a]Present address: School of Mechanical and Advanced Materials Engineering, UNIST, Korea.
[b]Author to whom correspondence should be addressed. Electronic mail: sangkoog@snu.ac.kr.

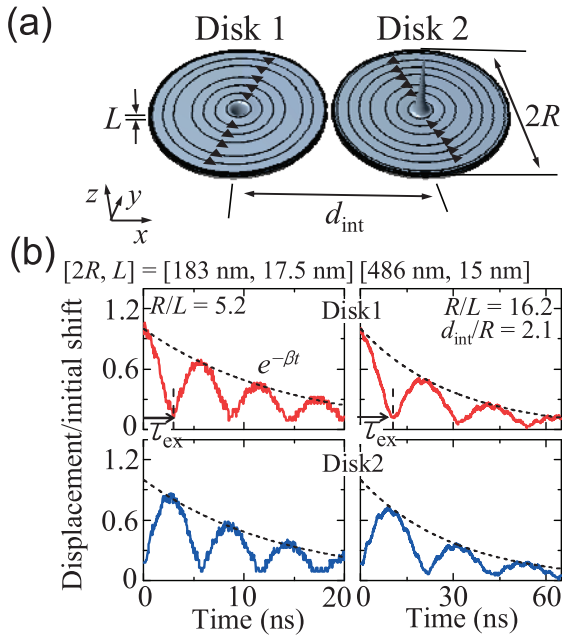

FIG. 1. (a) Geometrical configuration of two vortex-state disks of diameter $2R$, thickness L, and center-to-center interdistance d_{int}. The in-plane curling magnetization orienation of the two vortex-state disks is indicated, by the streamlines with the small arrows, as CCW for both disks. The upward and downward spikes at the core regions correspond to the upward and downward core magnetizations, respectively. (b) Displacements of vortex-core motions in both disks as function of time during relaxation process for indicated $[2R, L]$ dimensions in case of $d_{int}/R = 2.1$.

where $\mathbf{X}_{1,2} = (x_{1,2}, y_{1,2})$is the vortex-core position vector from the center of each of the disks (noted by the subscripts 1 and 2), $\mathbf{G}_{1,2} = -Gp_{1,2}\hat{\mathbf{z}}$ is the gyrovector with a constant $G = 2\pi LM_s/\gamma > 0$, and $\hat{D} = D\hat{I}$ is the damping tensor with the identity matrix $\hat{I}$ along with the damping constant $D = -\alpha\pi LM_s[2 + \ln(R/R_c)]/\gamma$ with the core radius R_c (Ref. 24). $W(\mathbf{X}_1, \mathbf{X}_2)$ is the potential energy of an entire coupled system, and thus can be expressed as the sum of the potential energy $W(0)$ at $\mathbf{X}_{1,2} = (0,0)$ and the potential energy $\frac{1}{2}\kappa(\mathbf{X}_1^2 + \mathbf{X}_2^2)$ for the shifted cores with the identical stiffness coefficient κ for isolated disks, and the last interaction term W_{int}. Considering the side-surface charges of each disk of a shifted core according to the rigid vortex model, W_{int} is given as $C_1C_2(\eta_x x_1x_2 - \eta_y y_1y_2)$, as reported in Ref. 18, where $\eta_{x,y}$ is the interaction strength coefficient along the x and y axes for a given material and dimensions. From previous experimental,[13,21,25] micromagnetic numerical,[13] and theoretical[18,20] studies, it is known that the dipolar interaction strength between two vortices depends strongly on d_{int}: Shibata *et al.*[18] reported the relation of $\eta_{x,y} \propto (d_{int}/R)^{-6}$ and Sukhostavets *et al.*[20] reported $\eta_{x,y} \propto (d_{int}/R)^{-3.2}$ for a range of $d_{int}/R = 2 - 5$.

Here, we will discuss the results of micromagnetic numerical calculations on the dynamic behaviors of coupled vortex oscillators under free relaxation for different dimensions. Typical oscillatory displacements at a characteristic periodicity with decreasing amplitude, as a function of time, and the mutual exchange of their local maxima and minima between the two disks, are clearly apparent, as shown in Fig. 1(b). From these data, we can extract τ_{ex} and β. As we defined in Ref. 13, the τ_{ex}, indicated by the black arrow, is the time period required for complete transport of the vortex gyration in one oscillator to the other one. The value of τ_{ex} is thus given as one-half of the displacement modulation periodicity, that is, as $\pi/|\Delta\omega|$, where $|\Delta\omega|$ is the frequency splitting that occurs by dipolar interaction between the shifted cores of the two disks.

On the other hand, the gradual decrease of the oscillatory displacements, represented by the dotted lines, can be expressed in the $e^{-\beta t}$ form using the attenuation coefficient term β. The amplitude attenuation is related to the energy loss during mutual gyration transfer between the two dots. From the simulation results, as shown in Fig. 1(b), we can extract the numerical values of τ_{ex} and β for the given material parameters of α and M_s and dimensions ranging from $R = 61.5$ to 243 nm, $L = 7.5$ to 40 nm, and $d_{int} = 9$ to 24 nm, as shown in Figs. 2 and 3 (see the symbols). The relative polarization configuration of p_1p_2 ($= +1$ for parallel core orientations, -1 for antiparallel ones) is also variable.

Prior to addressing the underlying physics of the simulation results for τ_{ex} and β shown in Figs. 2 and 3, we analytically derived both parameters to gain physical insights into the simulation results. Frist, τ_{ex} is reported to be given by $\pi/|\Delta\omega|$ (Ref. 13). Thus, it is necessary to obtain an explicit form of $|\Delta\omega|$. To do so, we adopted the representation of two normal modes for coupled vortex oscillators, $\mathbf{\Xi} = (x_1 + x_2, y_1 + p_1p_2y_2)$ and $\mathbf{\Omega} = (x_1 - x_2, y_1 - p_1p_2y_2)$ (Ref. 19), along

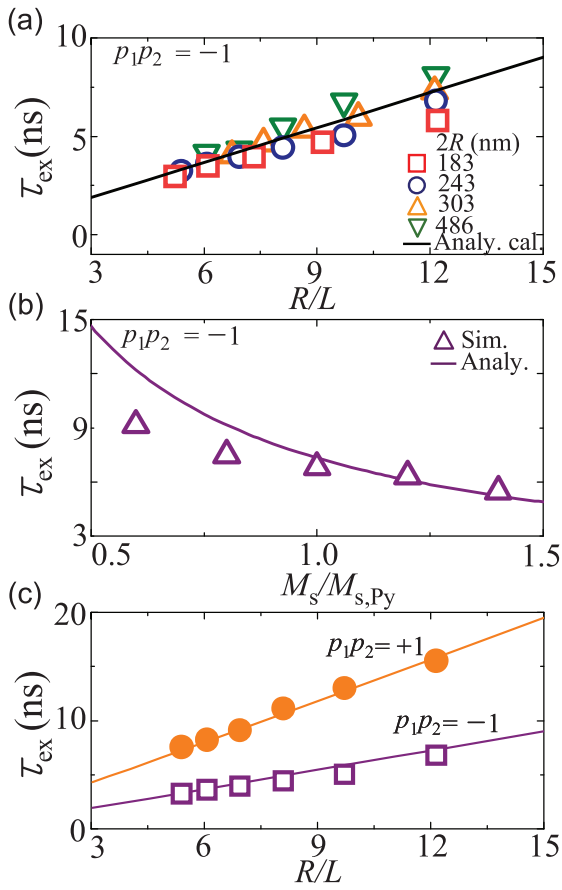

FIG. 2. (a) Vortex-gyration transfer rate τ_{ex} as function of ratio of R/L for different values of $2R$ with fixed value of $d_{int}/R = 2.1$ in case of $p_1p_2 = -1$. (b) τ_{ex} versus $M_s/M_{s,Py}$ for $[2R, L] = [243$ nm, 10 nm] and $p_1p_2 = -1$. (c) Comparison of variation of τ_{ex} with R/L for antiparallel ($p_1p_2 = -1$: purple) and parallel ($p_1p_2 = +1$: orange) polarization configurations in case of $2R = 243$ nm. In (a)–(c), the solid lines and symbols correspond to the analytical calculation and micromagnetic simulation results, respectively.

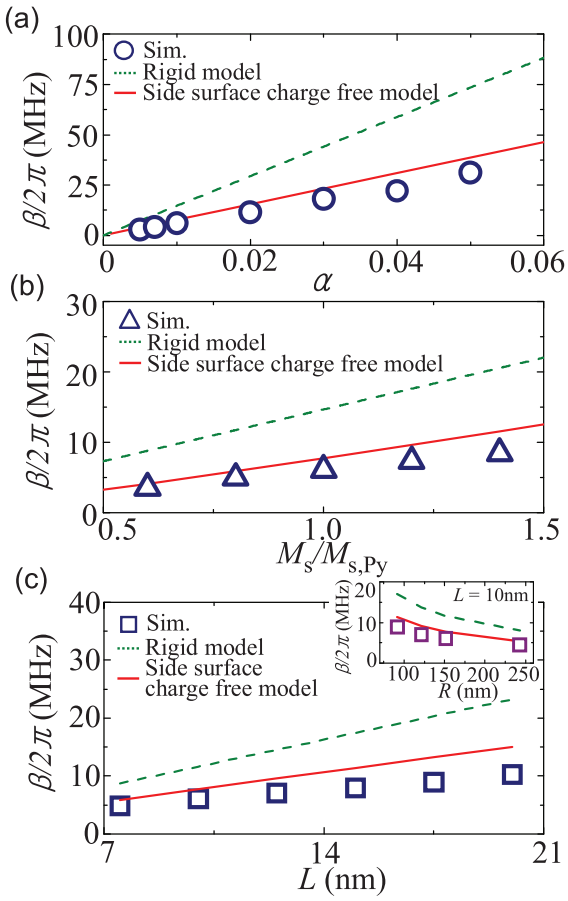

FIG. 3. Plots of $\beta/2\pi$ (a) versus α, (b) versus $M_s/M_{s,Py}$ for $[2R, L] = [303\,\text{nm}, 10\,\text{nm}]$, and (c) versus L. The open symbols correspond to the micromagnetic simulation results, while the dotted and solid lines represent the analytical calculation results for the rigid vortex model and side-surface-charge free model, respectively. The inset shows $\beta/2\pi$ versus R for a given $L = 10\,\text{nm}$ value.

with the corresponding eigenfrequencies $\tilde{\omega}_\Xi \approx \omega_0\sqrt{(1+\Gamma_x)(1-\Gamma_y)} - i\beta$ and $\tilde{\omega}_\Omega \approx \omega_0\sqrt{(1-\Gamma_x)(1+\Gamma_y)} - i\beta$, where $\omega_0 = \kappa/G$, $\Gamma_x = C_1C_2\eta_x/\kappa$ and $\Gamma_y = C_1C_2p_1p_2\eta_y/\kappa$, for cases of $G \gg |D|$ and $\eta_{x,y} \ll \kappa$. On the basis of the two normal coordinates, $|\Delta\omega|$ can be expressed simply as $|\text{Re}(\tilde{\omega}_\Xi) - \text{Re}(\tilde{\omega}_\Omega)|$and, thus, $\tau_{ex} \approx \pi G/|\eta_x - p_1p_2\eta_y|$. From the integration of $\eta_{x,y}$, we have explicit forms, $\eta_{x,y} = (\mu_0/8\pi)M_s^2(L^2/R)I_{x,y}$ with μ_0 the vacuum permeability, along with $I_{x,y}$ (which is a function of d_{int}/R and has a constant value for a given (d_{int}/R) range), and $I_x > I_y$ (for details, see Ref. 26). The explicit form of τ_{ex} is finally obtained as

$$\tau_{ex} \approx \frac{16\pi^3}{\mu_0\gamma M_s|I_x - p_1p_2I_y|}\left(\frac{R}{L}\right). \tag{2}$$

We can know from Eq. (2) that τ_{ex} varies dominantly with d_{int}, given the relation of $I_x \propto (d_{int}/R)^{-3.4}$ and $I_y \propto (d_{int}/R)^{-4.0}$, and for the case of $p_1p_2 = -1$, τ_{ex} thus decreases significantly with decreasing d_{int}. Also, τ_{ex} is inversely proportional to M_s and is linearly proportional to R/L. For example, the analytical calculation of τ_{ex} for the given values of $p_1p_2 = -1$, $M_s = M_{s,Py}$, and $d_{int}/R = 2.1$ is shown in Fig. 2(a). Figure 2(b) indicates that the value of τ_{ex} decreases with increasing M_s, and Fig. 2(c) plots the dependence of τ_{ex} versus R/L for the relative polarization configurations (i.e., $p_1p_2 = \pm 1$). The analytical data were in good agreement with the micromagnetic simulations. A relatively large deviation of τ_{ex} between the analytical and simulation results at smaller M_s was related to deviations of both G and $1/|\eta_x + \eta_y|$, but in this case, it was a product mainly of the deviation of $1/|\eta_x + \eta_y|$.

We stress here that the large difference in τ_{ex} between $p_1p_2 = +1$ and -1 within a wide range of R/L promises manipulation of signal propagation speed by variation of the switchable polarization states for the given dimensions, constituent material, and interdistance. The physical origin of such a dependence can be thought to be directly related to the frequency splitting caused by the modification of the stiffness of isolated disks' potential energy through their dipolar interaction. The values of M_s, R/L, $I_{x,y}$ (a function of d_{int}), and p_1p_2 influence the dipolar interaction and hence the potential energy stiffness of isolated disks: the larger the M_s and the smaller the d_{int}, the greater stiffness of the potential energy; and the larger the R/L, the less stiffness. Moreover, $p_1p_2 = -1$ yields stronger dipolar interaction than $p_1p_2 = +1$, since the opposite rotational senses of the gyrations in both disks, with their antiparallel polarities, result in stronger dipolar interaction than does the same rotational sense. The fact that τ_{ex} varies with R/L, M_s, and p_1p_2 provides a robust way to control and further reduce τ_{ex} (thereby effecting a faster processing speed) by varying those values.

The magnitude of coefficient β represents the degree of energy attenuation during signal propagation. β is given analytically as $\beta = -\kappa D/(G^2 + D^2) = -(D/G)\omega_0$ by solving Eq. (1) through its diagonalization with respect to the normal-mode coordinates.[19] For cases of $L \ll R$, using $\omega_0 \approx 10\gamma M_s(L/R)/3$ for the rigid model,[17,27] β is given simply as $\beta \approx \frac{5}{3}\alpha\gamma M_sL[2 + \ln(R/R_c)]/R$. As for the side-surface-charge free model, β can be expressed as $\beta \approx \frac{10}{9}\alpha\gamma M_sL[2 + \ln(R/R_c)]/R$ using $\omega_0 \approx 20\gamma M_s(L/R)/9$ (Ref. 27). These analytical forms allow us to understand the relation of energy loss to the given material parameters and dimensions during vortex-gyration transfer. In Fig. 3, we plotted the analytical calculations (lines) of β (for both the rigid and surface-charge-free models) compared with the micromagnetic simulation results (symbols). The analytical calculation (dotted lines) for the rigid vortex model is quite different from the micromagnetic simulation (open symbols), whereas the analytical calculation (solid lines) for the surface-charge-free-model is in better agreement with the simulation. The reason for such large deviation for the rigid model is the large deviation of ω_0 used for the analytical calculation from ω_0 for the realistic simulation case. The most important point to be addressed here is that β is a linear function of α, M_s, and L, and rather a complex function of R. According to the results shown in Fig. 3, a decrease in M_s and L and an increase in R allow for reduction in β while effecting an increase of τ_{ex}. Since α is related to β but not to τ_{ex}, while keeping τ_{ex} faster, β can be reduced by decreasing α and by optimizing the dimensions of the coupled dots. For example, the energy attenuation in transferring vortex gyrations from disk 1 to disk 2 can be represented by the ratio of the first maxima of the displacement of disk 2's vortex core to that of disk 1, $|\mathbf{X}_2|_{t=\tau_{ex}}/|\mathbf{X}_1|_{t=0} = e^{-\beta\cdot\tau_{ex}}$(Ref. 28). For the given case of

$M_s = M_{s,Py}$, and $[2R, L] = [303\ \text{nm}, 10\ \text{nm}]$, we obtained $|\mathbf{X}_2|_{max1}/|\mathbf{X}_1|_{max1} = 0.7529$ for $\alpha = 0.01$, but 0.8448 for $\alpha = 0.005$, leading to a 12% further reduction in the amplitude attenuation.

In conclusion, we demonstrated by both analytical derivations and micromagnetic simulations that a shorter τ_{ex} can be achieved by choosing a smaller R/L along with antiparallel polarizations and a larger M_s. Smaller β values can be obtained with intrinsic low-damping material and/or by using smaller M_s and thickness. Signal propagation speed and reduction of energy loss can be optimized by engineering the material parameters and dimensions of constituent disks and their compensation. This work provides a promising foundation for signal-processing speed enhancement and energy-loss reduction in vortex-gyration-transfer-based information-signal processing.

This work was supported by the Basic Science Research Program through the National Research Foundation of Korea (NRF) funded by the Ministry of Education, Science and Technology (Grant No. 20120000236).

[1]K. Bernstein, R. K. Cavin, W. Porod, A. Seabaugh, and J. Welser, Proc. IEEE **98**, 2169 (2010).
[2]R. P. Cowburn and M. E. Welland, Science **287**, 1466 (2000).
[3]I. Imre, G. Csaba, L. Ji, A. Orlov, G. H. Bernstein, and W. Porod, Science **311**, 205 (2006).
[4]D. B. Carlton, N. C. Emley, E. Tuchfeld, and J. Bokor, Nano Lett. **8**, 4173 (2008).
[5]D. A. Allwood, G. Xiong, M. D. Cooke, C. C. Faulkner, D. Atkinson, N. Vernier, and R. P. Cowburn, Science **296**, 2003 (2002).
[6]T. Schneider, A. A. Serga, B. Leven, B. Hillebrands, R. L. Stamps, and M. P. Kostylev, Appl. Phys. Lett. **92**, 022505 (2008).
[7]K.-S. Lee and S.-K. Kim, J. Appl. Phys. **104**, 053909 (2008).
[8]S.-K. Kim, J. Phys. D: Appl. Phys. **43**, 264004 (2010).
[9]A. Khitun, M. Bao, and K. L. Wang, J. Phys. D: Appl. Phys. **43**, 264005 (2010).
[10]K.-S. Lee, D.-S. Han, and S.-K. Kim, Phys. Rev. Lett. **102**, 127202 (2009).
[11]V. V. Kruglyak, S. O. Demokritov, and D. Grundler, J. Phys. D: Appl. Phys. **43**, 264001 (2010).
[12]H. Jung, Y.-S. Yu, K.-S. Lee, M.-Y. Im, P. Fischer, L. Bocklage, A. Vogel, M. Bolte, G. Meier, and S.-K. Kim, Appl. Phys. Lett. **97**, 222502 (2010).
[13]H. Jung, K.-S. Lee, D.-E. Jeong, Y.-S. Choi, Y.-S. Yu, D.-S. Han, A. Vogel, L. Bocklage, G. Meier, M.-Y. Im, P. Fischer, and S.-K. Kim, Sci. Rep. **1**, 59 (2011).
[14]S. Barman, A. Barman, and Y. Otani, IEEE Trans. Magn. **46**, 1342 (2010).
[15]A. Vogel, T. Kamionka, M. Martens, A. Drews, K. W. Chou, T. Tyliszczak, H. Stoll, B. Van Waeyenberge, and G. Meier, Phys. Rev. Lett. **106**, 137201 (2011).
[16]A. Vogel, M. Martens, M. Weigand, and G. Meier, Appl. Phys. Lett. **99**, 042506 (2011).
[17]K. Y. Guslienko, B. A. Ivanov, V. Novosad, Y. Otani, H. Shima, and K. Fukamichi, J. Appl. Phys. **91**, 8037 (2002).
[18]J. Shibata, K. Shigeto, and Y. Otani, Phys. Rev. B **67**, 224404 (2003).
[19]K.-S. Lee, H. Jung, D.-S. Han, and S.-K. Kim, J. Appl. Phys. **110**, 113903 (2011).
[20]O. V. Sukhostavets, J. M. Gonzalez, and K. Y. Guslienko, Appl. Phys. Express **4**, 065003 (2011).
[21]S. Sugimoto, Y. Fukuma, S. Kasai, T. Kimura, A. Barman, and Y. Otani, Phys. Rev. Lett. **106**, 197203 (2011).
[22]See http://math.nist.gov/oommf for the OOMMF code.
[23]A. A. Thiele, Phys. Rev. Lett. **30**, 230 (1973); D. L. Huber, Phys. Rev. B **26**, 3758 (1982).
[24]K. Y. Guslienko, Appl. Phys. Lett. **89**, 022510 (2006).
[25]A. Vogel, A. Drews, T. Kamionka, M. Bolte, and G. Meier, Phys. Rev. Lett. **105**, 037201 (2010).
[26]$\eta_{x,y}$ are expressed in integrated form as $\eta_x = \mu_0 M_s^2 R \int dz_1 dz_2 d\phi_1 d\phi_2 [\sin\phi_1 \sin\phi_2 / K(\phi_1, z_1, \phi_2, z_2)]/(8\pi)$ and $\eta_y = \mu_0 M_s^2 R \int dz_1 dz_2 d\phi_1 d\phi_2 [\cos\phi_1 \cos\phi_2 / K(\phi_1, z_1, \phi_2, z_2)]/(8\pi)$, where ϕ_i is a polar angle measured at the center of disk i from the x-axis, and $K(\phi_1, z_1, \phi_2, z_2) = [(d_{int}/R)^2 + 2(d_{int}/R)(\cos\phi_2 - \cos\phi_1) + 2 - 2\cos(\phi_2 - \phi_1) + (z_2 - z_1)^2]^{\frac{1}{2}}$. The integrations of $\eta_{x,y}$ range from 0 to L for $z_{1,2}$ and from 0 to 2π for $\phi_{1,2}$. From the results of the numerical integration of $\eta_{x,y}$ for the various geometrical parameters L, R, and d_{int}, it was found that $\eta_{x,y} = (\mu_0/8\pi) M_s^2 (L^2/R) I_{x,y}$, where $I_{x,y} > 0$ are functions only of d_{int}/R for the range $d_{int}/R = 2$–3.5, $I_x \propto (d_{int}/R)^{-3.4}$, and $I_y \propto (d_{int}/R)^{-4.0}$.
[27]K. Y. Guslienko, X. F. Han, D. J. Keavney, R. Divan, and S. D. Bader, Phys. Rev. Lett. **96**, 067205 (2006).
[28]$\beta \cdot \tau_{ex}$ is given analytically as $\beta \cdot \tau_{ex} \approx \frac{160}{9} \pi^3 \alpha [2 + \ln(R/R_c)]/(\mu_0 |I_x - p_1 p_2 I_y|)$.